catalysts

MDPI

Article

Catalytic Performance of Co_3O_4 on Different Activated Carbon Supports in the Benzyl Alcohol Oxidation

Misael Cordoba [1,2], Cristian Miranda [1], Cecilia Lederhos [2], Fernando Coloma-Pascual [3], Alba Ardila [4], Gustavo A. Fuentes [5], Yannick Pouilloux [6] and Alfonso Ramírez [1,*]

1 Grupo de Catálisis, Universidad del Cauca, Popayán 190001, Colombia; mcordoba@fiq.unl.edu.ar (M.C.); miranda.cristian@correounivalle.edu.co (C.M.)
2 Instituto de Investigaciones en Catálisis y Petroquímica, INCAPE (FIQ-UNL, CONICET), Santa Fe 3000, Argentina; clederhos@fiq.unl.edu.ar
3 Servicios Técnicos de Investigación, Facultad de Ciencias, Universidad de Alicante, E.03080 Alicante, Spain; f.coloma@ua.es
4 Research Group in Environmental Catalysis and Renewable Energies, Facultad de Ciencias Básicas Sociales y Humanas, Politécnico Colombiano Jaime Isaza Cadavid, Medellín 050001, Colombia; anardila@elpoli.edu.co
5 Departamento IPH, Universidad A. Metropolitana—Iztapalapa, México DF 09340, Mexico; gfuentes@xanum.uam.mx
6 Institute de Chimie des Milieux et des Matériaux de Poitiers, Université de Poitiers, 86000 Poitiers, France; yannick.pouilloux@univ-poitiers.fr
* Correspondence: aramirez@unicauca.edu.co; Tel.: +57-8-20-9900 (ext. 2339)

Received: 22 September 2017; Accepted: 7 October 2017; Published: 12 December 2017

Abstract: Co_3O_4 particles were supported on a series of activated carbons (G60, CNR, RX3, and RB3). Incipient wetness method was used to prepare these catalysts. The effect of the structural and surface properties of the carbonaceous supports during oxidation of benzyl alcohol was evaluated. The synthetized catalysts were characterized via IR, TEM, TGA/MS, XRD, TPR, AAS, XPS, and N_2 adsorption/desorption isotherm techniques. Co_3O_4/G60 and Co_3O_4/RX3 catalysts have high activity and selectivity on the oxidation reaction reaching conversions above 90% after 6 h, without the presence of promoters. Catalytic performances show that differences in chemistry of support surface play an important role in activity and suggest that the presence of different ratios of species of cobalt and oxygenated groups on surface in Co_3O_4/G60 and Co_3O_4/RX3 catalysts, offered a larger effect synergic between both active phase and support increasing their catalytic activity when compared to the other tested catalysts.

Keywords: benzyl alcohol; oxidation; activated carbon; cobalt oxide; heterogeneous catalysts

1. Introduction

The oxidation of alcohols to aldehydes or ketones is one of the most important transformations in fine chemical industry [1] due to the versatility of the carbonyl group [2]. Various traditional reagents, such as Cr and Mn oxides [3], have been used as catalysts, but as a result of their high toxicity and/or poor atom economy [4], has promoted the search of other kind of oxidants. Sheldon [5] describes the capability of molecular oxygen (O_2) or hydrogen peroxide (H_2O_2) as oxidant agents, which are environmental friendly. On this way many works have using these oxidants with supported metals such as Pd [6], Pt [7], Rh [8] and Ru [9] as catalysts during the oxidation reactions. Although these catalysts have showed important catalytic results, their high cost is the main problem. Thus, searching for an alternative to the noble metal catalysts, supported Cu [10], Mn [11], Ni [12], or Co [13] oxides has been proposed in the aerobic oxidations of alcohols. Within these "low cost" catalyst series, the cobalt-based solids have exhibited high catalytic activity. In this case, the role of the Co_3O_4

nanoparticles focus in the dehydrogenation of alcohols because they can provide Lewis acid sites [14]. Xiaoyuan et al. [15] developed a hybrid composite of cobalt based framework exhibited excellent catalytic performance in selective oxidation of benzyl alcohol by using molecular oxygen. This catalyst reaches an 89.5% alcohol conversion and 97.3% selectivity to benzaldehyde. Xiao et al. [16] prepared a "sandwich" N-doped graphene/Co_3O_4 hybrid catalyst, which performed well catalytic efficiency for alcohols conversion. It is well know that the structure and property of the active phase in the catalysts are affected for the material used as the support. The study of the support effect on the catalytic performance in all the reactions is very important [17]. Qiao et al. [18] observed a better behavior with catalysts of Co_3O_4 supported on hydrotalcite.

It has been noticed that Co_3O_4 nanoparticles supported on activated carbon (AC) were highly active for benzyl alcohol oxidation to the corresponding aldehyde. Zhu et al. obtained a 100% benzyl alcohol conversion to 3 h and selectivity of 87.3% to benzaldehyde, they have showed that the presence of oxygen species from functional groups of the AC surface might participate in the reaction and those are subsequently regenerated by oxygen present in the reaction environment [14,19]. Despite the previous use of Co_3O_4 supported on AC, little information is available in the literature regarding, in particular, the effect of the structural and surface properties of the carbonaceous supports. It has not been much discussed the interaction between both the AC surface and Co_3O_4 nanoparticles in the oxidation reactions of benzyl alcohol. Thus in this work, four commercial AC from different origin (G60, CNR, RX3, and RB3), were used as support and the cobalt oxide was deposited on them. The incipient wetness method to obtain four catalysts different Co_3O_4/G60, Co_3O_4/RX3, Co_3O_4/CNR, and Co_3O_4/RB3 was used. The effect of the structural and surface properties of Co_3O_4/AC-type catalysts during the benzyl alcohol oxidation reaction was evaluated.

2. Results and Discussion

2.1. Characterization of the Supports and Catalysts

Figure 1A exhibit the XRD profiles of the activated carbons used as supports. The patterns show that all of the AC samples might be mostly amorphous. However, the CNR and G60 carbons are presented as a mixture of amorphous and crystalline graphitic phases, evidenced by the diffraction observed at about 27° (2θ) [20], which was confirmed by transmission electron microscopy (TEM). Co_3O_4/AC catalysts have a crystalline phase identified as a cobalt oxide spinel, which is very active for the reaction studied here [14,19]. Figure 1B shows the characteristic XRD peaks of Co_3O_4 on G60, at 2θ ≈ 19° ((111) face), 31.2° ((220) face), 36.8° ((311) face), 44.8° ((400) face), 59.3° ((511) face), and 65.2° ((440) face).

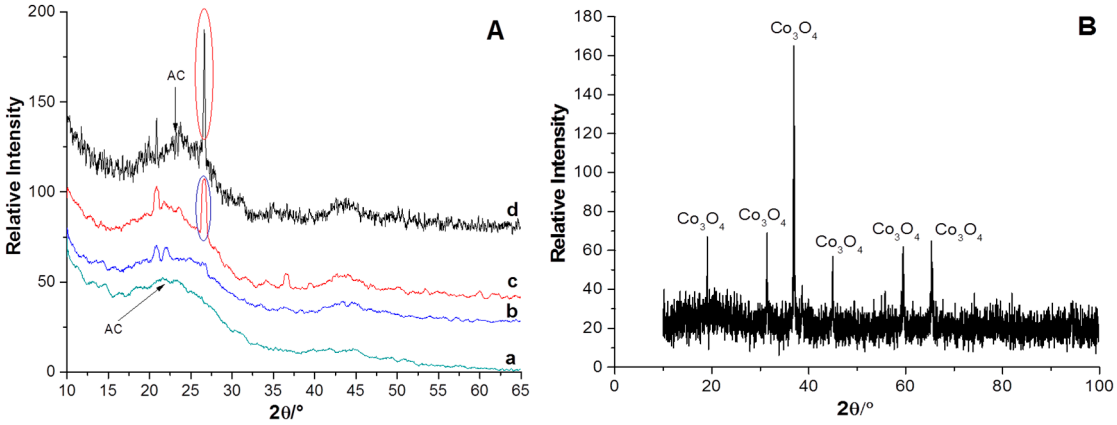

Figure 1. XRD of (**A**) supports: (**a**) RB3, (**b**) RX3, (**c**) G60 and (**d**) CNR; and (**B**) Co_3O_4/G60 catalyst.

Table 1 summarizes the surface area (S_{BET}), adsorption parameters (Vμ: micropore) calculated from the N_2 adsorption isotherms, the average pore diameter, TPR, and XPS results for all supports. As expected [20,21], all the samples present high S_{BET} values, between 900 and 1500 $m^2\ g^{-1}$ [22,23] being the highest for RX3 and CNR. All of the supports show differences in the total pore volume caused by their differences in the manufacturing method. G60 and CNR have the larger values of V_S. Notably, G60 has a significantly larger average pore size, while the other supports present lower and similar values.

Table 1. Physicochemical properties, TPR and XPS results of the activated carbon (AC) support.

Sample	S_{BET} ($m^2\ g^{-1}$)	V_μ ($cm^3\ g^{-1}$)	Pore Size (nm)	TPR		XPS
				Area [(a)]	T_{max} (°C) [(b)]	BE O 1s (eV)
G60	978	0.336	41.1	41,159	680	531.2–532.9
RB3	1133	0.520	24.3	38,296	696	531.2–532.9
RX3	1524	0.622	26.7	42,368	688	531.3–533.1
CNR	1503	0.680	24.4	39,707	739	531.3–533.3

[(a)] Area under the peaks from hydrogen consumption (deconvolution); [(b)] Maximum temperature of the main peak.

For H_2-TPR results of AC, a broad peak for each support with maximum between 680 and 740 °C was observed. According to Table 1, the H_2-TPR curves had similar T_{max} but for the CNR sample shifted to 50 °C, indicating that CNR support has functional groups, which are reduced with greater difficulty. Those hydrogen consumptions observed at high temperatures are assigned to the support reduction and the presence of impurities [24,25]. Area under the peaks from hydrogen consumption estimates an amount of reducible species from several groups present on support surface, specially oxygenated such as phenol, carboxyl, and carbonyl groups, etc.; as well as nitrogen containing groups. Thereby, a slight difference in area under the peaks was observed, being highest for the RX3 and G60 supports.

IR spectra for all carbonaceous supports are presented in Figure 2A. Surface differences of supports were also observed in the IR characterization. All of the supports present the same signals between 3447 and 1621 cm^{-1}, assigned to bond stretching vibrations (O–H) of the carboxylic hydroxyl group. Vibrations of carbonyl group (C=O) occurring between 1700 and 800 cm^{-1}, and vibration of ether, lactones, phenols, and epoxide groups occurring in the region between 1500 and 700 cm^{-1} [26–28] were found. In Figure 2B, intensities of these signals differed between the activated carbon samples, indicating that the concentration of several functional groups on the surface, are quite different. IR analysis of the catalysts indicates that there are changes in functional groups on the AC surface as a result of cobalt oxide deposition. Furthermore, bands at 572 and 664 cm^{-1}, which correspond to the stretching vibration of Co–O in cobalt oxide [29,30], are very strong in the case of the G60-based material. The intensity of the characteristic IR vibration bands for carbonyl, quinone, and carboxyl groups decreased upon the incorporation of cobalt oxide onto each support is made, presumably as a result of the functional groups-cobalt oxyhydroxide species interaction during the impregnation and calcination steps [22]. The Thermogravimetric Analysis/Mass Spectrometry (TGA/MS) profile of all carbonaceous supports is presented in Figure 3. From the CO and CO_2 desorption, as the temperature is increased, it is possible to obtain information about the different superficial groups present on the support [31,32]. In Figure 3B, the CO desorption peaks show an evolution from 700 to 1000 °C mainly for the RX3, G60, and RB3 supports, which could be attributed to carbonyl and quinone groups [31,32].

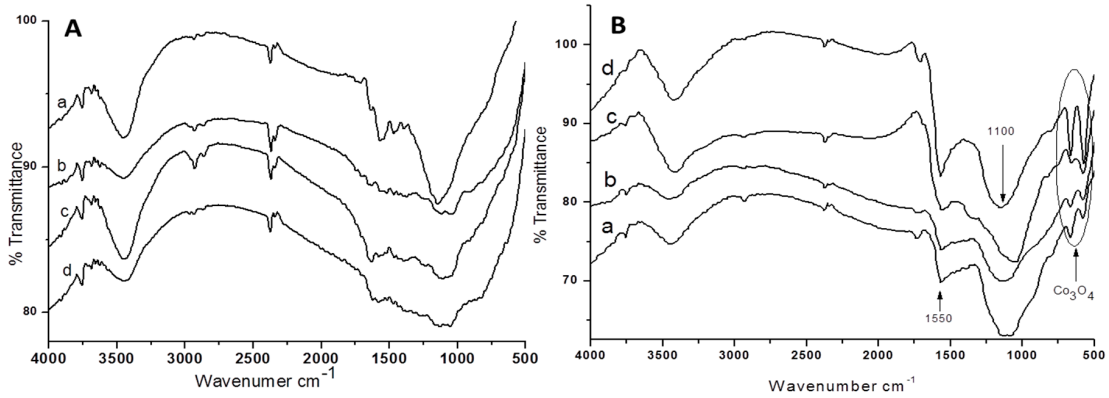

Figure 2. IR spectra of (**A**) supports: (**a**) G60, (**b**) RX3, (**c**) RB3, and (**d**) CNR; (**B**) catalysts: (**a**) Co_3O_4/RB3, (**b**) Co_3O_4/RX3, (**c**) Co_3O_4/CNR, (**d**) Co_3O_4/G60.

The CNR carbonaceous support shows two peaks in CO desorption with two maximum at 676 and 971 °C, which are related with the presence of phenol, ether, carbonyl/quinone, and anhydride groups on the surface, indicating that this support have weaker groups. In Figure 3A, CO_2 evolution with different intensities and peaks are shown for each support. Initially, a peak from 150 to 450 °C is assigned to carboxylic acid groups; for temperatures below 400–650 °C, a characteristic peak of carboxylic anhydride groups protrudes; also from 600 to 900 °C a final peak is observed generated from anhydrides and lactone groups, which are more stable systems [33]. The G60, RX3, and CNR supports present throughout the analysis the greatest intensity peaks when compared with the RB3 support profile, which is less intense, indicating differences in quantity, nature, and thermal stability of functional groups of the supports.

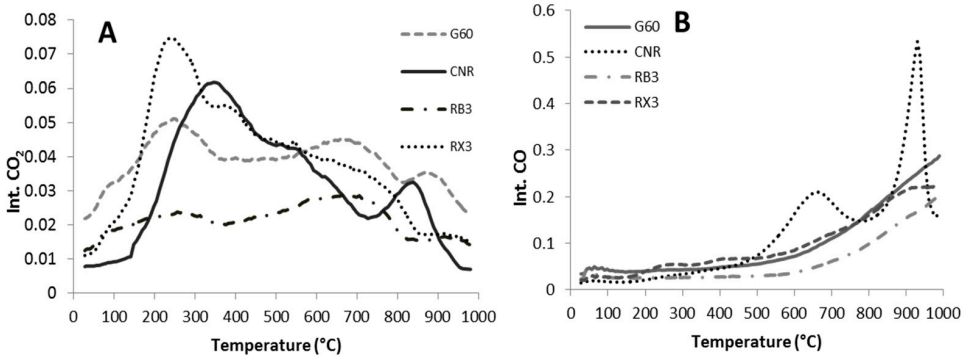

Figure 3. TGA/MS of AC supports. (**A**) Desorption of CO_2 and (**B**) Desorption of CO.

The total areas of CO, CO_2, and O_2 obtained by TGA/MS analysis deconvolution for the AC supports are shown in Table 2. By comparing the results is possible to see that the CNR, RX3, and G60 supports have greater amount of functional groups compared to RB3 support. It is important to know the amount of functional groups present in support, their both decomposition and stability, because those groups can interact with the active phase Co_3O_4 and with molecular oxygen. This promotes the generation of active oxygen species, superoxide, and peroxides mainly, which will interfere in the oxidation reaction of alcohols [14,34,35]. These analyses are consistent largely with the IR analysis and TPR-H_2 (Table 1).

Table 1 and Figure 4A present O1s BE values and spectra for the carbonaceous supports. From the deconvolution of O 1s XPS spectra, it is possible to obtain additional information about the nature of the surface oxygen groups on each support. All of the AC supports present two peaks at ca. 531 and 533 eV, which are representative of the typical C=O groups. The first peak is attributed to the oxygen atoms in carbonyl, esters, amides, and anhydrides groups; while, the second peak is associated to the oxygen atoms

in ether, esters, and anhydrides groups [27,36]. In Figure 4A can be noted that both G60 and RX3 supports have similar spectra, being the peak at 531 eV the most intense; by contrast, it is observed for RB3 where the highest peak is at 533 eV, it may indicate high presence of carboxyl groups, while the CNR support has similar intensities in these two peaks, indicating that this support has equivalent quantities of those groups.

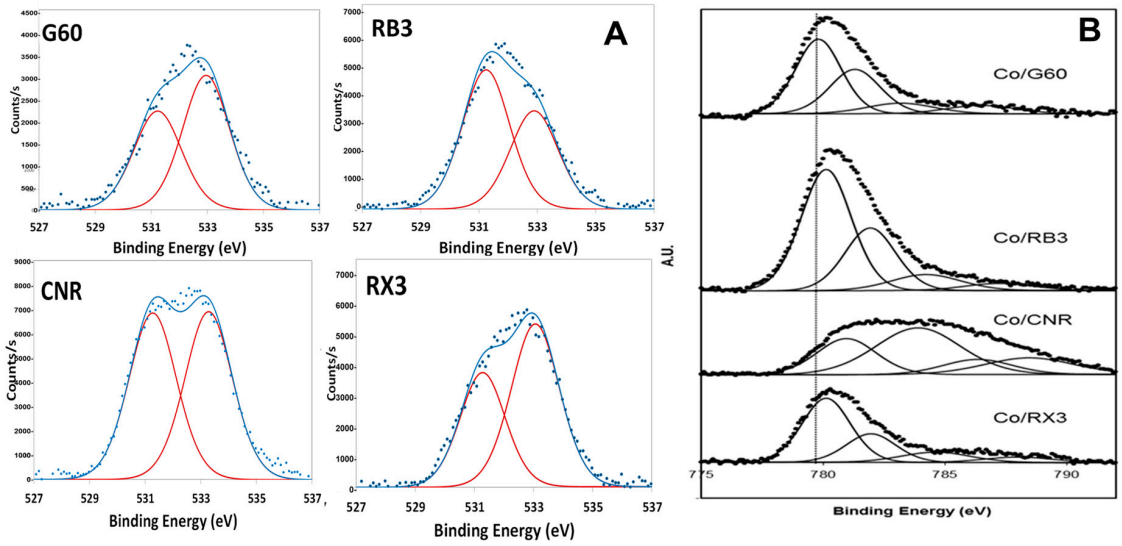

Figure 4. (**A**) O1s BE spectra by XPS of the supports: G60, RB3, RX3 and CNR; (**B**) XPS spectra for BE Co $2p_{3/2}$ of the catalysts: Co/G60, Co/RB3, Co/RX3 and Co/CNR.

Table 2. Total area of CO, CO_2 and O_2 obtained by TGA/MS deconvolution of the AC supports.

Sample	CO (μmol/g)	CO_2 (μmol/g)	O_2 (μmol/g)	Total Area
G60	91.0	37.2	16.6	144.8
RB3	55.9	20.6	11.7	88.2
RX3	94.1	36.9	16.9	147.9
CNR	115.6	30.3	9.9	155.8

Morphological differences in the AC samples were also identified via TEM. As shown in Figure 5, RX3, RB3, and G60 carbons (Figure 5A–C, respectively) are amorphous, whereas TEM of CNR (Figure 5D) shows a graphite structure throughout the activated carbon, in agreement with the XRD analysis Figure 1A.

Table 3 presents the BET (Brunauer–Emmett–Teller) surface area values, metal loading, and XPS results for the catalysts under study. All of the samples exhibited a decrease in S_{BET} values as compared to the respective activated carbon values as a result of pore clogging by cobalt species. It was observed that the loading of cobalt varied among the different samples. It is known that the differences in support surface chemistry have a profound effect at every stage of catalyst preparation [26] and played an important role affecting the impregnation of Co species.

H_2-TPR analysis of the catalysts (Figure 6) shows the presence of very similar peaks for each supports with differences in the intensity for each peak. The reduction of the species of cobalt indicates the presence of Co_3O_4, initially a peak around 250–350 °C is attributed to the reduction of Co_3O_4 to CoO; later, a second peak around 400–500 °C attributed to the reduction of CoO to Co^0 [37]. Similarly, it is observed a peak around 500 °C, attributed to methane produced by AC supports hydrogenation due to the catalytic influence of the catalysts themselves [38,39]. These results are according to TPR analysis, indicating the presence of both Co_3O_4 and CoO species during the oxidation reaction conditions. In addition, this analysis allows obtaining further information about the amount of functional groups present in the catalysts, by measuring the peak area for all around 600–900 °C (Table 3). It is clear that the amount of functional groups in the catalysts is decreased as follows: Co_3O_4/G60 > Co_3O_4/RX3

> Co_3O_4/RB3 > Co_3O_4/CNR; this tendency is maintained after the thermal treatment during the synthesis, which is similar to the characterization results of the supports by H_2-TPR and TGA/MS.

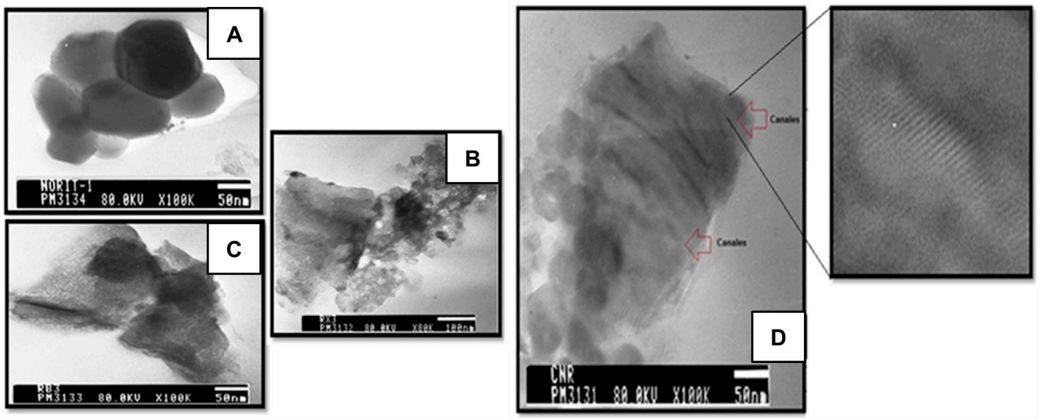

Figure 5. Transmission electron microscopy (TEM) images of AC supports: (**A**) G60; (**B**) RX3; (**C**) RB3; and, (**D**) CNR.

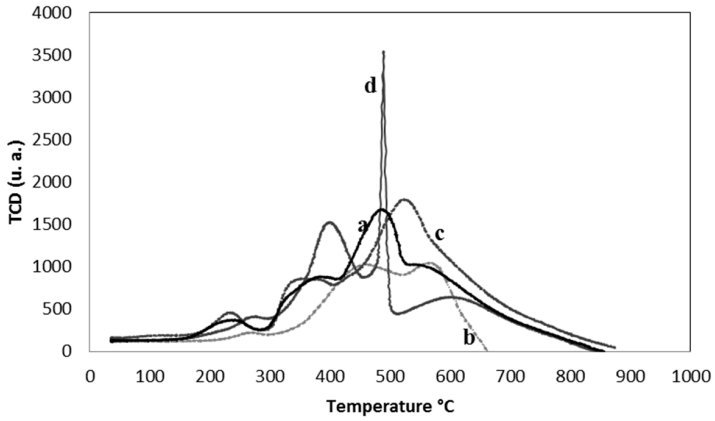

Figure 6. H_2-TPR profiles of Catalyst. (**a**) Co_3O_4/G60; (**b**) Co_3O_4/CNR; (**c**) Co_3O_4/RB3; and, (**d**) Co_3O_4/RX3.

Table 3. Metal loading, BET surface area, H_2-TPR and XPS results of the catalysts.

Catalyst	S_{BET} (m^2 g^{-1})	Metal Loading (wt %)	TPR Area [a]	XPS			
				BE Co $2p_{3/2}$ (eV)	Co^{3+}/Co^{2+} (at./at.)	Co/C (at./at.)	BE O 1s (eV)
Co_3O_4/G60	777	15.2	202,855	779.9 781.4	1.07	0.041	530.2 532.1
Co_3O_4/RB3	452	8.4	114,036	779.8 781.3	0.99	0.092	529.9 531.5 533.3
Co_3O_4/RX3	1007	10.8	129,193	779.9 781.2	0.62	0.033	530.3 532.1
Co_3O_4/CNR	969	9.8	66,562	780.6 782.4	0.56	0.044	531.2 533.4 535.3
Co_3O_4/G60 Used Catalyst	729	9.5	200,025	779.9 781.7	1.28	0.046	530.3 532.1 534.0

[a] Area under the peaks of AC from hydrogen consumption (deconvolution).

Surface properties of the catalysts were investigated via XPS. In all of the samples, three peaks for the Co $2p_{3/2}$ signal were detected. According to the literature [40], peaks at 779.5 and 780.8 eV correspond to Co^{3+} and Co^{2+} species, respectively. All of the supported catalysts present both binding energy corresponding to Co^{3+} and Co^{2+} species in Co_3O_4 and CoO compounds. These results agree with TPR analysis, indicating the presence of both Co_3O_4 and CoO species during the oxidation reaction conditions. The XPS spectra for BE Co $2p_{3/2}$ for catalysts after deconvolution are shown in Figure 4B. The third signal detected by XPS is observed in Figure 4B at 784.7 eV corresponds to the shake-up satellite of the Co $2p_{3/2}$ species, observed in compounds such as $Co(NO_3)_2$, Co_3O_4, Co_2O_3, and CoO [29]. The Co^{3+}/Co^{2+} superficial atomic ratio for all of the supported catalysts is shown in Table 3. The CoO_x/G60 catalyst has the largest surface atomic ratio, indicating a larger concentration of Co^{3+} species on the catalyst surface. When RB3 is used as support, the amount of Co^{3+} and Co^{2+} surface species is similar. The Co/C surface atomic ratio was used as a measure of Co surface dispersion. The largest value was observed with Co_3O_4/RB3, while the other samples had less dispersion. This assignment has to be taken cautiously, because it cannot be ensured that all Co species are being detected by XPS. The deconvolution of O 1s signal, low values can be seen at 529–530 eV, corresponding to O^{2-} species of Co_3O_4 and CoO. The different values for the O 1s peak (Table 3) from 531 to 535 eV in all of the catalysts could be assigned to the oxygen in the surface groups of the carbon support such as carbonyl (or quinone), anhydride (or lactone), and carboxyl groups, according to Figueiredo et al. [27]. The XPS results of all of the catalysts show three peaks for the C 1s signal at ca. 284.3 eV, 285.1 eV, and 286.4 eV. The first peak could be associated to graphitic carbon, while the last two peaks correspond to C=O, C=C, CNH_2, COH, and COC signals [40]. It is known that the carbons surface is usually complex, present several groups, specially oxygenated and also nitrogen-containing groups. The surface chemistry of these supports is usually modified during the preparation of supported catalysts, and it may affect the surface dispersion of the active phase.

2.2. Catalytic Tests

In Figure 7, the total conversion values as a function of time for all catalysts in study are shown. The different Co_3O_4/AC catalysts were tested in the partial oxidation reaction of benzyl alcohol to produce benzaldehyde. In this figure, Co_3O_4 unsupported active phase, AC and the blank without catalyst were also evaluated. Blank and all AC support-only reactions lead practically the same conversion (6 to 7–10%, respectively; after 6 h of reaction). The conversion in the presence of unsupported active phase, Co_3O_4, in an amount equivalent the cobalt oxide impregnated on the AC supports was 48.7%. The catalytic properties of cobalt oxide are due mainly to its Lewis acid nature [14]. Additionally, several reports [14,41,42] indicate that the Co_3O_4 oxide systems used as catalysts in oxidation reactions and described in the literature have a spinel structure, which is conformed with both Co^{+2} and Co^{+3} ions. However, the high catalytic activity of the spinel in oxidation processes is related to the weaker Co(III)-O bond, i.e., to the higher oxidation state of the cation [41]. Conversion values of 100%, 90.2%, 76.4%, and 66.2% after 6 h of reaction were obtained using Co_3O_4/G60, Co_3O_4/RX3, Co_3O_4/CNR, and Co_3O_4/RB3 catalysts, respectively.

The Co_3O_4/RX3, Co_3O_4/RB3 catalysts, and Co_3O_4 showed catalysts deactivation, it process could be attributed to the presence of water product of the reaction or decrease in oxidation in the catalytic system. Bartholomew [43] indicates that the oxidation of the metal phase by water leads to the formation of inactive metallic oxides and to the sintering of the active phase due to the presence of water. Selectivity to benzaldehyde was 99% at 40% of conversion in all of the cases (Table 4) but the presence of benzoic acid was observed after the total conversion in the most active catalyst (Co_3O_4/G60).

Furthermore, the catalyzed reaction by Co_3O_4/RB3, Co_3O_4/CNR, and Co_3O_4/RX3 presents an induction period that lasts between 30 min and 1 h. This could be attributed to several factors involving the cobalt species and the support, the results of XPS (Table 3) we observe that the atomic ratio Co^{+3}/Co^{+2}, are 0.99, 0.56, and 0.62 for the catalysts Co_3O_4/RB3, Co_3O_4/CNR, and Co_3O_4/RX3, respectively. These values are variable for the species of cobalt showing that the cobalt species +2

is greater what could generate some period of induction. This phenomenon could be occurring because Co species are in a non-active phase, and during the first minutes the reaction conditions lead to its activation. The work of F.X. Llabrés i Xamena et al. [44] showed that the use of the cobalt catalyst (Co^{2+}/MOFs) involves a long induction period for the tetralin oxidation reaction. It could be suggested that some cobalt need activation during the reaction conditions but some additional research is necessary to reach a better understanding about this induction time on the catalytic behavior of the catalysts studied.

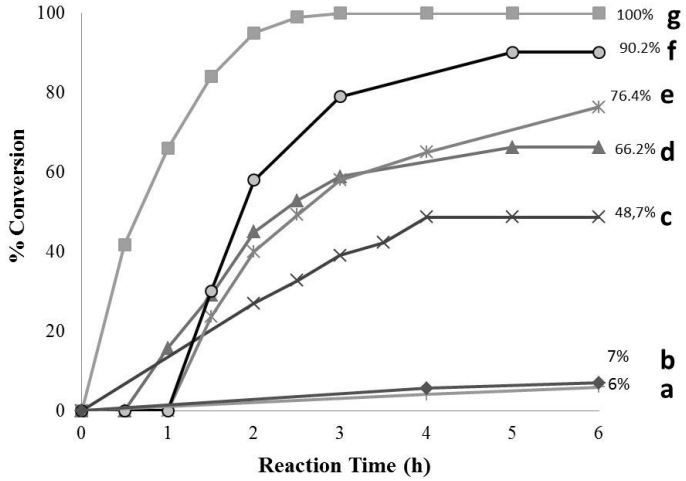

Figure 7. Benzyl alcohol conversion as a function of reaction time: (**a**) Without catalyst, (**b**) AC, (**c**) Co_3O_4, (**d**) Co_3O_4/RB3, (**e**) Co_3O_4/CNR, (**f**) Co_3O_4/RX3, and (**g**) Co_3O_4/G60.

All of the catalysts have good results in catalytic oxidation of benzyl alcohol to benzaldehyde. When comparing the results of catalytic oxidation of the active phase and the activated carbon supports, 48% and 7–10% conversion, respectively, we observed that all four catalysts evaluated have better catalytic performance in this reaction with synergism between Co_3O_4 and AC, its activity decreases as follows:Co_3O_4/G60 > Co_3O_4/RX3 > Co_3O_4/CNR > Co_3O_4/RB3 (Table 4). The catalysts with higher activity are those supported on G60 and RX3 activated carbons, while the catalysts synthetized with supports CNR and RX3 showed lower activity, the catalysts from G60 and RX3 supports were those with the largest content of surface functional groups based on TPR and TPD analysis (Tables 1–3). In this order, it may be attributed to the properties found in the supports and properties of the impregnated active phase.

When considering that the active phase content in each catalyst is different, these values are normalized by finding the catalytic activity with respect to the cobalt loading (Tables 3 and 4). It could be demonstrated that the best catalytic behavior was for Co_3O_4/G60 during the oxidation reaction of benzyl alcohol, which could be associated to the highest presence of Co^{3+} superficial species (Co^{3+}/Co^{2+} atomic ratio = 1.07), detected by XPS, and the high presence of functional groups on this catalyst, while Co_3O_4/RB3 catalyst showed a lower activity having a similar amount of Co^{+3} (Co^{3+}/Co^{2+} atomic ratio = 0.99) but with a lower presence of functional groups, indicating less synergism between both support and active phase. In the same way, conversions demonstrated the same tendency in the catalytic performance for Co_3O_4/RX3 and Co_3O_4/CNR. The enhanced activity stems in part from synergetic effect between Co_3O_4 and AC, when compared to the unsupported oxide and the AC tested individually. These results suggest that the differences in surface chemistry of AC supports such as amount of groups, morphology, and texture, and also the amount, type and ratio of cobalt species impregnated led to changes in the catalysts, and thus to different activities.

Reusability of the Co_3O_4/G60 catalyst for the benzyl alcohol oxidation reaction was studied. After the first use in reaction the catalyst was filtered, washed, calcined, and recycled once.

Total conversion decreased ca. 10%, while the selectivity to benzyl alcohol remains above 99% during the recycle run although a loss of Co loading (ca. 37%) on catalyst was observed (Table 4). The XPS analysis (Table 3) from fresh and used Co_3O_4/G60 catalyst showed no significant change in the Co $2p_{3/2}$ BE position. A slight increase in the area under the Co peak that corresponds to Co^{3+} species in the used catalyst is noted. A small increase in the Co/C superficial atomic ratio was observed in the used catalyst, according to the AAS results.

Table 4. Catalytic activity of Co_3O_4/AC catalysts.

System	Conversion (%) *	Selectivity (%) *	Cobalt (wt %)	Catalytic Activity (mmol BA $h^{-1}g_{Co}^{-1}$)
Co_3O_4	48.7	≥99	-	-
Co_3O_4/G60	100	≥99	15.2	4.2
Co_3O_4/RX3	90.1	≥99	10.8	3.4
Co_3O_4/CNR	76.3	≥99	9.8	0.25
Co_3O_4/RB3	66.5	≥99	8.4	0.30
Co_3O_4/G60 (Used Catalyst)	89	≥99	9.5	3.1

* Selectivity to 40% of reaction.

3. Materials and Methods

3.1. Catalyst Preparation

Four commercial AC were used as supports in this study: G60 (steam-activated carbon produced by Darco), RX3 Extra (acid-washed steam-activated carbon, from Norit), CNR115 (phosphoric acid activated carbon, from Norit), and RB3 (steam-activated extruded carbon, from Norit). All activated carbons were purchased from the CABOT Corporation (Boston, MA, USA). The supports were macerated and sieved to a particle size of 100 µm and all of the supports were not modified with oxidizing agents. Impregnation of cobalt on the support was performed by the incipient wetness method as follows: 0.5 g of $Co(NO_3)_2{\cdot}6H_2O$ (Merck, 99.9%) (Merck, Darmstadt, Germany) were dissolved in 5 mL of water and then 1 g of AC (G60, RX3, CNR or RB3) was added to the solution. The mixture was then dried in air at 110 °C for 12 h. The resulting solid was treated under He flow during 2 h at 350 °C (heating rate of 5 °C min^{-1}). Co_3O_4 unsupported active phase was used in a comparative way. This was synthesized with the same conditions with which the catalysts were prepared.

3.2. Catalyst Characterization

BET surface areas were measured by N_2 physisorption at −196 °C with a Micromeritics Flowsorb II 2300. Infrared spectra (IR) (400–4000 cm^{-1}) were obtained by using a Nicolet IR-200 instrument (Thermo Fisher Scientific, Waltham, MA, USA) in transmission mode. TEM images were obtained by an electron microscope JEOL 1200EX (JEOL, Tokyo, Japan) operating at 90 kV. X-ray Diffraction (XRD) was measured in a RIGAKU Miniflex II diffractometer (Rigaku, Tokyo, Japan), using Cu Kα radiation (λ = 1.5405 Å) at 15 mA and 30 kV, in the $10° < 2\theta < 65°$ range, and a scan speed of 2° min^{-1}. The metal loading was determined by Atomic Absorption Spectroscopy (AAS) in Thermo-Electron series S equipment (Thermo Fisher Scientific, Waltham, MA, USA). Surface chemistry were quantified in DTA/TGA-TA Instruments SDT Q600 (TA Instrument, New Castle, DE, USA) coupled to a Hiden Mass Spectrometer 0–200 amu, temperature program from 25 to 1000 °C and a ramp of 20 °C min^{-1} in He atmosphere at a flow of 100 mL min^{-1}. Temperature-Programmed Reduction with H_2 (H_2-TPR) were measured using 10% H_2/Ar as a reducing gas in a Micromeritics Autochem II 2920 (Micromeritics, Norcross, GA, USA). The gas flow rate was 25 mL min^{-1} and flow controllers at 10 °C min^{-1}. Calibration was made with CuO 99%, Merck (Merck, Darmstadt, Germany). The area under the peaks from hydrogen consumption was determined by the deconvolution using

the Fityk programme. XPS measurements were acquired in a VG-Microtech Multilab equipment (VG-Microtech, East Grinstead, UK) with a MgKα (hν: 1253.6 eV) radiation source, passing energy of 50 eV and pressure of 5×10^{-7} Pa. A careful deconvolution of the spectra was made and the areas of the peaks were estimated by calculating the integral of each peak after subtracting a Shirley background and fitting the experimental peak to a combination of Lorentzian/Gaussian lines of 30–70% proportions.

3.3. Catalytic Tests

The oxidation of benzyl alcohol was carried out in a glass stirred semi-batch reactor provided with a thermometer and a reflux condenser. Catalytic tests were performed by using 0.2 mMol of benzyl alcohol (Merck, 99.5%), 20 mL of toluene used as solvent (Merck, 99.9%), 0.1 g of catalyst, 750 rpm to eliminate the external diffusional limitations, and an O_2 stream of 50 mL min^{-1} at 80 °C for 6 h. Reactant and products were analyzed with a Shimadzu GC14A Gas Chromatograph (Shimadzu, Tokyo, Japan) equipped with a Flame Ionization Detector and a Varian VF-1 capillary column. To get an idea of the reusability of the catalysts, after the reaction the solid catalysts were removed from the reaction mixture by filtration, and then washed and dried at 100 °C for 1 h. Finally, the solid was calcined at 400 °C in an inert stream during 2 h and used again in reaction.

4. Conclusions

Co_3O_4 particles were deposited on four AC supports with different physical-chemical properties. These catalysts were evaluated in the partial oxidation of benzyl alcohol and compared with unsupported Co_3O_4. The unsupported active phase Co_3O_4 that resulted was less active than the supported oxide, showing that it is important in the distribution, ratio, type, and amount of Co species on the activated carbon support, because the physical-chemical properties of AC as a support have a direct impact over the oxide.

The four catalysts have good results in the conversion of benzyl alcohol, and all of them showed high selectivity toward benzaldehyde (>99%), the desired product of the partial oxidation reaction. The catalyst prepared with Co_3O_4 particles over G60 and RX3 supports are more active for benzyl alcohol oxidation reaction with activity values of 4.2 and 3.4 mmol BA h^{-1} $g_{Co}{}^{-1}$, respectively. The highest concentration of surface oxygen functionalities and the best physical-chemical properties in the catalysts can help in increasing the activity in the alcohol oxidation. Nevertheless, additional research is necessary to reach a better understanding about the effect of support on the catalytic behavior of the catalysts studied. For the Co_3O_4/G60 catalyst, the reusability during the partial oxidation of benzyl alcohol was studied. After the first cycle of reaction, the total conversion decreases ca. 10%, while selectivity to desired product values was relatively constant.

Acknowledgments: The author acknowledges the financial support from University of Cauca (project ID VRI 3573). M. Cordoba thanks COLCIENCIAS (Young Researchers Program 2012-Call 566), the Research Institute of Catalysis and Petrochemistry—INCAPE (Argentina), Design of Advanced Catalytic Materials Group, Department of Process Engineering, Universidad Autónoma Metropolitana—Iztapalapa, UAM-I (Mexico), and the group of Zeolites and Solids from Université de Poitiers (France).

Author Contributions: Alfonso Ramírez conceived the project. Misael Cordoba, Cristian Miranda, Fernando Coloma-Pascual, Alba Ardila, Yannick Pouilloux, Cecilia Lederhos and Gustavo A. Fuentes performed the experiments and Support and Catalysts Characterization. Alfonso Ramírez, Misael Córdoba, Cecilia Lederhos, Alba Ardila and Cristian Miranda wrote the final manuscript.

Conflicts of Interest: The authors declare no conflict of interest.

References

1. Larock, R.C. *Comprehensive Organic Transformations*; CVH: New York, NY, USA, 1999; pp. 1234–1250.
2. Zhan, B.-Z.; Thompson, A. Recent developments in the aerobic oxidation of alcohols. *Tetrahedron* **2004**, *60*. [CrossRef]

3. Deshpande, S.S.; Jayaram, R.V. Liquid phase catalytic oxidation of alcohols over mixed metal oxides. *Catal. Commun.* **2008**, *9*, 186–193. [CrossRef]
4. Steves, J.E.; Stahl, S.S. Copper-Catalyzed Aerobic Alcohol Oxidation. In *Liquid Phase Aerobic Oxidation Catalysis: Industrial Applications and Academic Perspectives*; Wiley-VCH Verlag GmbH & Co. KGaA: Berlin, Germany, 2016; pp. 85–96.
5. Arends, I.W.C.E.; Sheldon, R.A. Modern Oxidation of Alcohols Using Environmentally Benign Oxidants. In *Modern Oxidation Methods*; Wiley-VCH Verlag GmbH & Co. KGaA: Berlin, Germany, 2010; pp. 147–185.
6. Villa, A.; Wang, D.; Dimitratos, N.; Su, D.; Trevisan, V.; Prati, L. Pd on carbon nanotubes for liquid phase alcohol oxidation. *Catal. Today* **2010**, *150*, 8–15. [CrossRef]
7. Korovchenko, P.; Donze, C.; Gallezot, P.; Besson, M. Oxidation of primary alcohols with air on carbon-supported platinum catalysts for the synthesis of aldehydes or acids. *Catal. Today* **2007**, *121*, 13–21. [CrossRef]
8. Wang, B.; Lin, M.; Ang, T.P.; Chang, J.; Yang, Y.; Borgna, A. Liquid phase aerobic oxidation of benzyl alcohol over Pd and Rh catalysts on N-doped mesoporous carbon: Effect of the surface acido-basicity. *Catal. Commun.* **2012**, *25*, 96–101. [CrossRef]
9. Yang, X.; Wang, X.; Qiu, J. Aerobic oxidation of alcohols over carbon nanotube-supported Ru catalysts assembled at the interfaces of emulsion droplets. *Appl. Catal. A Gen.* **2010**, *382*, 131–137. [CrossRef]
10. Cruz, P.; Pérez, Y.; del Hierro, I.; Fajardo, M. Copper, copper oxide nanoparticles and copper complexes supported on mesoporous SBA-15 as catalysts in the selective oxidation of benzyl alcohol in aqueous phase. *Microporous Mesoporous Mater.* **2016**, *220*, 136–147. [CrossRef]
11. Tang, Q.; Huang, X.; Chen, Y.; Liu, T.; Yang, Y. Characterization and catalytic application of highly dispersed manganese oxides supported on activated carbon. *J. Mol. Catal. A Chem.* **2009**, *301*, 24–30. [CrossRef]
12. Punniyamurthy, T.; Velusamy, S.; Iqbal, J. Recent Advances in Transition Metal Catalyzed Oxidation of Organic Substrates with Molecular Oxygen. *Chem. Rev.* **2005**, *105*, 2329–2364. [CrossRef] [PubMed]
13. Taghavimoghaddam, J.; Knowles, G.P.; Chaffee, A.L. Preparation and characterization of mesoporous silica supported cobalt oxide as a catalyst for the oxidation of cyclohexanol. *J. Mol. Catal. A Chem.* **2012**, *258*, 79–88. [CrossRef]
14. Zhu, J.; Faria, J.L.; Figueiredo, J.L.; Thomas, A. Reaction Mechanism of Aerobic Oxidation of Alcohols Conducted on Activated-Carbon-Supported Cobalt Oxide Catalysts. *Chem. A Eur. J.* **2011**, *17*, 7112–7117. [CrossRef] [PubMed]
15. Yang, X.; Wu, S.; Hu, J.; Fu, X.; Peng, L.; Kan, Q.; Huo, Q.; Guan, J. Highly efficient N-doped magnetic cobalt-graphene composite for selective oxidation of benzyl alcohol. *Catal. Commun.* **2016**, *87*, 90–93. [CrossRef]
16. Nie, R.; Shi, J.; Du, W.; Ning, W.; Hou, Z.; Xiao, F.-S. A sandwich N-doped graphene/Co_3O_4 hybrid: An efficient catalyst for selective oxidation of olefins and alcohols. *J. Mater. Chem. A* **2013**, *1*, 9037–9045. [CrossRef]
17. Pan, C.-J.; Tsai, M.-C.; Su, W.-N.; Rick, J.; Akalework, N.G.; Agegnehu, A.K.; Cheng, S.-Y.; Hwang, B.-J. Tuning/exploiting Strong Metal-Support Interaction (SMSI) in Heterogeneous Catalysis. *J. Taiwan Inst. Chem. Eng.* **2017**, *74*, 154–186. [CrossRef]
18. Qiao, D.; Xu, C.; Xu, J. Aerobic oxidation of benzyl alcohol over Co_3O_4/rehydrated hydrotalcite catalysts: The promotional effect of hydrotalcite support. *Catal. Commun.* **2014**, *45*, 44–48. [CrossRef]
19. Zhu, J.; Kailasam, K.; Fischer, A.; Thomas, A. Supported Cobalt Oxide Nanoparticles As Catalyst for Aerobic Oxidation of Alcohols in Liquid Phase. *ACS Catal.* **2011**, *1*, 342–347. [CrossRef]
20. Shi, P.; Su, R.; Wan, F.; Zhu, M.; Li, D.; Xu, S. Co_3O_4 nanocrystals on graphene oxide as a synergistic catalyst for degradation of Orange II in water by advanced oxidation technology based on sulfate radicals. *Appl. Catal. B Environ.* **2012**, *123–124*, 265–272. [CrossRef]
21. Onoe, T.; Iwamoto, S.; Inoue, M. Synthesis and activity of the Pt catalyst supported on CNT. *Catal. Commun.* **2007**, *8*, 701–706. [CrossRef]
22. Francisco, R.-R. The role of carbon materials in heterogeneous catalysis. *Carbon* **1998**, *36*, 159–175. [CrossRef]
23. Auer, E.; Freund, A.; Pietsch, J.; Tacke, T. Carbons as supports for industrial precious metal catalysts. *Appl. Catal. A Gen.* **1998**, *173*, 259–271. [CrossRef]
24. Krishna Murthy, J.; Chandra Shekar, S.; Siva Kumar, V.; Rama Rao, K.S. Highly selective zirconium oxychloride modified Pd/C catalyst in the hydrodechlorination of dichlorodifluoromethane to difluoromethane. *Catal. Commun.* **2002**, *3*, 145–149. [CrossRef]

25. Pinna, F.; Signoretto, M.; Strukul, G.; Benedetti, A.; Malentacchi, M.; Pernicone, N. Ruthenium as a Dispersing Agent in Carbon-Supported Palladium. *J. Catal.* **1995**, *155*, 166–169. [CrossRef]
26. Boonamnuayvitaya, V.; Sae-ung, S.; Tanthapanichakoon, W. Preparation of activated carbons from coffee residue for the adsorption of formaldehyde. *Sep. Purif. Technol.* **2005**, *42*, 159–168. [CrossRef]
27. Figueiredo, J.L.; Pereira, M.F.R.; Freitas, M.M.A.; Órfão, J.J.M. Modification of the surface chemistry of activated carbons. *Carbon* **1999**, *37*, 1379–1389. [CrossRef]
28. Zhuang, Q.L.; Kyotani, T.; Tomita, A. DRIFT and TK/TPD analyses of surface oxygen complexes formed during carbon gasification. *Energy Fuels* **1994**, *8*, 714–718. [CrossRef]
29. Christoskova, S.G.; Stoyanova, M.; Georgieva, M.; Mehandjiev, D. Preparation and characterization of a higher cobalt oxide. *Mater. Chem. Phys.* **1999**, *60*, 39–43. [CrossRef]
30. Tang, C.-W.; Wang, C.-B.; Chien, S.-H. Characterization of cobalt oxides studied by FT-IR, Raman, TPR and TG-MS. *Thermochim. Acta* **2008**, *473*, 68–73. [CrossRef]
31. Aksoylu, A.E.; Madalena, M.; Freitas, A.; Pereira, M.F.R.; Figueiredo, J.L. The effects of different activated carbon supports and support modifications on the properties of Pt/AC catalysts. *Carbon* **2001**, *39*, 175–185. [CrossRef]
32. Román-Martínez, M.C.; Cazorla-Amorós, D.; Linares-Solano, A.; de Lecea, C.S.-M. Tpd and TPR characterization of carbonaceous supports and Pt/C catalysts. *Carbon* **1993**, *31*, 895–902. [CrossRef]
33. Elodie, G.; Rodrigues, M.F.R.P.; Chen, X.; Delgado, J.J.; Órfão, J.J.M. Influence of activated carbon surface chemistry on the activity of Au/AC catalysts in glycerol oxidation. *J. Catal.* **2011**, *281*, 119–127.
34. Luo, J.; Yu, H.; Wang, H.; Wang, H.; Peng, F. Aerobic oxidation of benzyl alcohol to benzaldehyde catalyzed by carbon nanotubes without any promoter. *Chem. Eng. J.* **2014**, *240*, 434–442. [CrossRef]
35. Slot, T.K.; Eisenberg, D.; van Noordenne, D.; Jungbacker, P.; Rothenberg, G. Cooperative Catalysis for Selective Alcohol Oxidation with Molecular Oxygen. *Chem. A Eur. J.* **2016**, *22*, 12307–12311. [CrossRef] [PubMed]
36. Zielke, U.; Hüttinger, K.J.; Hoffman, W.P. Surface-oxidized carbon fibers: I. Surface structure and chemistry. *Carbon* **1996**, *34*, 983–998. [CrossRef]
37. Fu, T.; Jiang, Y.; Lv, J.; Li, Z. Effect of carbon support on Fischer–Tropsch synthesis activity and product distribution over Co-based catalysts. *Fuel Process. Technol.* **2013**, *110*, 141–149. [CrossRef]
38. Zhang, H.; Alhamed, Y.A.; Al-Zahrani, A.; Daous, M.; Inokawa, H.; Kojima, Y.; Petrov, L.A. Tuning catalytic performances of cobalt catalysts for clean hydrogen generation via variation of the type of carbon support and catalyst post-treatment temperature. *Int. J. Hydrog. Energy* **2014**, *39*, 17573–17582. [CrossRef]
39. Zhang, H.; Lancelot, C.; Chu, W.; Hong, J.; Khodakov, A.Y.; Chernavskii, P.A.; Zheng, J.; Tong, D. The nature of cobalt species in carbon nanotubes and their catalytic performance in Fischer-Tropsch reaction. *J. Mater. Chem.* **2009**, *19*, 9241–9249. [CrossRef]
40. National Institute of Standards and Technology. *NIST Standard Reference Database*; National Institute of Standards and Technology: Gaithersburg, MD, USA, 2007.
41. Christoskova, S.G.; Stojanova, M.; Georgieva, M.; Mehandzhiev, D. Study on the thermal stability of a high Co-oxide used as low-temperature catalyst and oxidant for complete oxidation. *Thermochim. Acta* **1997**, *292*, 77–83. [CrossRef]
42. Mate, V.R.; Shirai, M.; Rode, C.V. Heterogeneous Co_3O_4 catalyst for selective oxidation of aqueous veratryl alcohol using molecular oxygen. *Catal. Commun.* **2013**, *33* (Suppl. C), 66–69. [CrossRef]
43. Bartholomew, C.H. Mechanisms of catalyst deactivation. *Appl. Catal. A Gen.* **2001**, *212*, 17–60. [CrossRef]
44. Xamena, L.F.X.; Casanova, O.; Galiasso, T.R.; Garcia, H.; Corma, A. Metal organic frameworks (MOFs) as catalysts: A combination of Cu^{2+} and Co^{2+} MOFs as an efficient catalyst for tetralin oxidation. *J. Catal.* **2008**, *255*, 220–227. [CrossRef]

© 2017 by the authors. Licensee MDPI, Basel, Switzerland. This article is an open access article distributed under the terms and conditions of the Creative Commons Attribution (CC BY) license (http://creativecommons.org/licenses/by/4.0/).